J Hepatobiliary Pancreat Sci (2013) 20:206–213
DOI 10.1007/s00534-012-0576-9

ORIGINAL ARTICLE

Activation of alpha-smooth muscle actin-positive myofibroblast-like cells after chemotherapy with gemcitabine in a rat orthotopic pancreatic cancer model

Jun Yamao · Hideyoshi Toyokawa · Songtae Kim · So Yamaki · Sohei Satoi · Hiroaki Yanagimoto · Tomohisa Yamamoto · Satoshi Hirooka · Yoichi Matsui · A-Hon Kwon

Published online: 22 November 2012

Abstract
Background To investigate the behavior of activated pancreatic stellate cells (PSCs), which express alpha-smooth muscle actin (α-SMA), and pancreatic cancer cells in vivo, we examined the expression of α-SMA-positive myofibroblast-like cells in pancreatic cancer tissue after treatment with gemcitabine (GEM) using a Lewis orthotopic rat pancreatic cancer model.
Methods The effect of GEM on DSL-6A/C1 cell proliferation was determined by cell counting method. The orthotopic pancreatic cancer animals were prepared with DSL-6A/C cells, and treated with GEM (100 mg/kg/weekly, for 3 weeks). At the end of treatment, α-SMA expression, fibrosis, transforming growth factor (TGF)-β1 and vascular endothelial growth factor (VEGF) were evaluated by histopathological and Western blot analyses.
Results DSL-6A/C1 cell proliferation was significantly reduced by co-culturing with GEM in vitro. Survival time of pancreatic cancer animals (59.6 ± 13.4 days) was significantly improved by treatment with GEM (89.6 ± 21.8 days; $p = 0.0005$). Alpha-SMA expression in pancreatic cancer tissue was significantly reduced after treatment with GEM ($p = 0.03$), however, there was no significant difference in Sirius-red expression. Expression of VEGF was significantly reduced by GEM treatment, but the expression of TGF-β1 was not inhibited.
Conclusion GEM may suppress not only the tumor cell proliferation but also suppress PSCs activation through VEGF reduction.

Keywords Pancreatic cancer · Alpha-smooth muscle actin · Myofibroblast-like cell · Chemotherapy · Vascular endothelial growth factor

Introduction

Pancreatic cancer is a pathologically unique tumor that is composed of cancer cells and extremely dense desmoplasia containing extracellular matrix (ECM) protein, myofibroblast-like pancreatic stellate cells (PSCs), and inflammatory cells. Since their discovery in 1998, PSCs have been identified as the major source of ECM proteins found in chronic pancreatitis or pancreatic fibrosis in both experimental animals and humans [1–4]. Quiescent PSCs are activated by inflammatory cytokines or oxidative stress and transformed to myofibroblast-like cells (MCs), which express alpha-smooth muscle actin (α-SMA) [4, 5]. Activated PSCs show markedly increased ECM protein synthesis in response to various stimuli, such as cytokines and growth factors [5, 6].

There has been accumulating evidence of interaction between pancreatic cancer cells and PSCs. Pancreatic cancer cells induce PSC proliferation and ECM production. Conditioned medium from a pancreatic cancer cell line promotes the proliferation of PSCs [7]. Growth factors such as transforming growth factor (TGF)-β1, platelet-derived growth factor (PDGF), and fibroblast growth factor (FGF)-2 secreted by pancreatic cancer cells induce PSC activation [5]. However, most of these studies provided important evidence of stroma–tumor interactions through in vitro or subcutaneous tumor models.

J. Yamao · H. Toyokawa · S. Kim · S. Yamaki · S. Satoi (✉) · H. Yanagimoto · T. Yamamoto · S. Hirooka · Y. Matsui · A.-H. Kwon
Department of Surgery, Kansai Medical University, 2-3-1 Shin-machi, Hirakata, Osaka 573-1191, Japan
e-mail: satoi@hirakata.kmu.ac.jp

A recent study showed that activated PSCs may regulate the malignant behavior of pancreatic cancer cells [8]. Fujita et al. [9] investigated the significance of α-SMA expression in pancreatic cancer and the correlation between α-SMA mRNA levels and patient prognosis. Patients with high α-SMA expression had a significantly shorter survival. Thus, α-SMA-positive PSCs are thought to be strongly associated with growth and the microenvironment of pancreatic tumors.

The aim of this study was to investigate the relationship between activated PSCs and cancer cells in pancreatic tumors in vivo. We examined the expression of α-SMA, which is a marker of activated PSCs, in a clinically relevant rat orthotopic pancreatic cancer model after treatment with gemcitabine (GEM).

Materials and methods

Cell lines and culture

The rat ductal pancreatic adenocarcinoma cell line DSL-6A/C1 [10] was purchased from the American Type Culture Collection (Rockville, MD, USA), and cultured in Waymouth's MB 752/1 medium (Gibco, Grand Island, NY, USA). The cell culture medium was supplemented with 10 % heat-inactivated fetal bovine serum (FBS; Gibco), penicillin G (100 U/mL), and streptomycin (100 μg/mL). The cells were incubated in a humidified atmosphere of 5 % CO_2 at 37 °C.

DSL-6A/C1 cell proliferation assay

The effect of GEM on DSL-6A/C1 cell proliferation was determined by cell counting method. A total of 1×10^4 cells were incubated with or without GEM (Gemcitabine hydrochloride JD001, SYNCHEM OHG) at concentrations of 1.0 or 5.0 μM/L. The cell numbers relative to that on day 1 were counted on days 2, 4 and 7.

Laboratory animals

Five-week-old male Lewis rats (LEW/SsN Slc) weighing 100–150 g were purchased from Shimizu Laboratory Supplies Co., Ltd. (Kyoto, Japan). Animals were maintained in microisolator cages in a Specific Pathogen Free animal facility at the Kansai Medical University with autoclaved bedding, food, and water. The rats were maintained on a daily 12-h-light/12-h-dark cycle. All experiments were conducted in accordance with the national guidelines for the care and use of laboratory animals, and the experimental protocol was approved by the Animal Experimentation Committee, Kansai Medical University (No. 06-026).

Animal model of orthotopic pancreatic cancer

The Lewis rat orthotopic pancreatic cancer model was prepared as previously described, with modification [11]. A total of 10^6 DSL-6A/C1 cells were injected subcutaneously into the right flank of Lewis rats anesthetized with Isoflurane (Abbott Japan, Tokyo, Japan) inhalation. The subcutaneous tumors were excised under strict aseptic conditions, when they had reached a size of 15 mm in the largest diameter. The tumors were minced by a scalpel into small fragments of 1 mm^3 in size. Tumor recipient Lewis rats were also anesthetized with Isoflurane inhalation, and their abdomens were opened. Five small tissue pockets were prepared under a microscope in the pancreatic parenchyma as an implantation bed (OME-1000, Olympus, Tokyo, Japan). One tumor fragment was placed into each pancreatic tissue pocket in such a way that the tumor tissue was completely surrounded by pancreatic parenchyma. No sutures or fibrin glue were used to fix the tumor fragments to the recipient pancreas. The pancreas was relocated into the abdominal cavity, which was subsequently closed. Four weeks after orthotopic pancreatic tumor implantation, all animals were anesthetized, and tumor growth was confirmed by relaparotomy in the pancreatic parenchyma without distant metastasis.

Experimental model

All tumor-bearing animals were randomly divided into a control group (no treatment) and a GEM treatment group. The GEM treatment group animals were administered GEM (100 mg/kg) three times weekly through the penile vein. The control animals were administered saline.

Twelve animals in each group were followed for 120 days. Six in each group were sacrificed at 4 weeks for assays. At the time of sacrifice, pancreatic tumor tissue samples were fixed in 10 % buffered formalin for routine histopathology and immunohistochemistry and snap frozen for Western blot analysis.

Histopathological examinations

Routine histopathology

Initial hematoxylin and eosin staining was performed to choose tissue blocks that contained large enough areas of pancreatic carcinoma tissue. Normal pancreas and pancreatic carcinoma tissue were fixed in 10 % buffered formalin, embedded in paraffin, sectioned at 3 μm, and stained with hematoxylin and eosin.

Immunohistochemistry

Paraffin sections were rehydrated and washed in PBS for 5 min three times. Sections were incubated with 1 % H_2O_2 for 30 min to block endogenous peroxidases. To prevent nonspecific binding of antibody, sections were incubated for 30 min at room temperature with a blocking solution containing tris-buffered saline, 1 % bovine serum albumin, and 10 % goat serum. For immunohistochemical analysis, sections were incubated with primary antibody (monoclonal mouse anti-α-SMA antibody; Nichirei Bioscience, Tokyo, Japan) for 1 h at room temperature; monoclonal mouse anti-PCNA (Nichirei Bioscience, Tokyo, Japan) overnight at 4 °C, and then incubated with biotinylated secondary antibody at room temperature. The avidin–biotin–peroxidase immune complex was visualized with 3,3-diaminobenzidine tetrahydrochloride substrate chromogen system (DAKO, Botany, Australia). Sections were counterstained with Mayer's hematoxylin (Sigma) for 5 min.

Picrosirius red staining: The evaluation of fibrosis in the specimens of the four experimental groups was done by the Picrosirius red staining technique [12]. Picrosirius red staining can be used simply as a substitute for van Gieson's stain as a sensitive method for collagen staining. Following deparaffinization and hydration, the sections were stained with Sirius Red F3B (Alfa Aesar, MA, USA).

Quantitative color analysis for immunohistochemistry

The images were visualized with a Nikon ECLIPSE E1000 M microscope and photographed with a Nikon DIGITAL CAMERA DXM1200 (Nikon Corporation, Tokyo, Japan) using Lumina Vision software (version 2.2; Mitani Corporation, Tokyo, Japan). The area of positive immunostained regions per section was determined by computer assisted morphometry. A frame of 4 × 4 mm was marked over the carcinoma area for analysis. Tissues confined within this frame were then scanned automatically. Pictures were loaded individually onto the software interface and the color range of immunostained positive areas was evaluated. The results were expressed as the percentage of positive area in the total scanned surface and the means of the 12 analyzed photomicrographs per animal were calculated.

The number of PCNA-stained cancer cells was assessed by counting in a high-power field. The PCNA labeling index was determined as the percentage of the granulosa cell number with positively stained nuclei to the total cell number in the same fields [13]. The means of 12 randomly selected areas per section were calculated.

Western blot analysis of α-SMA, TGF-β1 and VEGF

Pancreatic tumor tissues (100 mg/rat) from control and experimental rats were minced and incubated on ice for 30 min in 1 mL of ice cold whole-cell lysate buffer (10 mM Tris–HCl, pH 7.4, containing 1 % Triton X-100, 0.5 % Nonidet P-40, 1 mM sodium orthovanadate, 1 mM phenylmethylsulfonylfluoride, and protease inhibitor cocktail, Roche Diagnostics, Mannheim, Germany). The minced tissue was homogenized (KINEMATICA POLYTRON PT1300D, Switzerland) and centrifuged at 16,000×*g* at 4 °C for 15 min. The proteins were then fractionated by SDS-PAGE, electrotransferred to PVDF membranes (Bio-Rad Lab., CA, USA), blotted with the following antibodies, and detected with an ECL blotting detection reagent (GE Healthcare Bio-sciences Corp., NJ, USA). Anti-α-SMA (diluted 1:1000), anti-TGF-β1 (Abcam, MA, USA) (diluted 1:2000) and anti-vascular endothelial growth factor (VEGF) (Santa Cruz Biotechnology, Inc., CA, USA) (diluted 1:200) were used as primary antibodies. β-Tubulin (internal control, CloneTUB2.1, Sigma, Saint Louis, USA) was used to verify equal loading. Experiments were repeated at least three times using different samples.

Statistical analysis

All experiments were performed three to five times. Data are presented as mean ± SEM. Data were analyzed for statistical significance by analysis of variance with post hoc Student's *t* test analysis. Differences in Kaplan–Meier survival curves were evaluated by the log-rank test. These analyses were performed with the assistance of a computer program (JMP 5 Software SAS Campus Drive, Cary, NC, USA). Differences were considered significant at $p < 0.05$.

Results

Effect of gemcitabine on DSL-6A/C1 cell proliferation

DSL-6A/C1 cells were cultured in complete medium to which was added 1.0 or 5.0 μM/L of GEM. DSL-6A/C1 cell proliferation was significantly reduced on day 7 in co-culture with 1.0 μM/L of GEM compared with the control ($p = 0.004$), and DSL-6A/C1 cell proliferation was almost completely blocked by 5.0 μM/L GEM (Fig. 1).

Orthotopic model of rat pancreatic cancer

Four weeks after orthotopic pancreatic tumor implantation, about 70 % of the animals had confirmed tumor growth in pancreatic parenchyma without visible distant metastasis

(Fig. 2a). The mean survival time of the control animals was 59.6 ± 13.4 days. Almost all the animals died from peritoneal dissemination with massive ascites. Histopathologic examination of the pancreatic tumors revealed moderately differentiated ductal-type adenocarcinomas (Fig. 2b).

Fibrosis in pancreatic tumor

Quiescent PSCs are activated and transformed to MCs, which express α-SMA and synthesize ECM. Alpha-SMA-positive MCs and fibrosis were histopathologically evaluated using anti-mouse-α-SMA antibody and Picrosirius red staining. Alpha-SMA-positive MCs and Picrosirius red-positive ECM were significantly increased in pancreatic tumor tissue compared with normal pancreas ($p = 0.005$) (Figs. 5d, 7c).

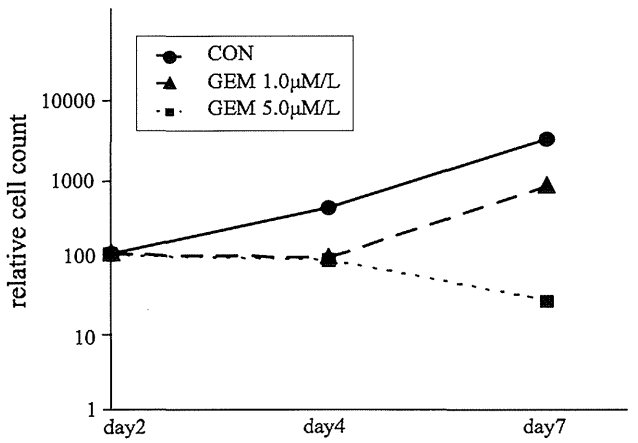

Fig. 1 The effect of GEM on DSL-6A/C1 cell proliferation. DSL-6A/C1 cell proliferation was significantly reduced in co-culture with GEM in a dose-dependent manner ($p = 0.004$). CON: without GEM (*black line*). GEM: 1.0 μM/L (*dashed line*) and 5.0 μM/L (*dotted line*) concentrations of GEM

In vivo anti-tumor effect of gemcitabine treatment

The mean animal survival time of the rat pancreatic cancer model (59.6 ± 13.4 days) was significantly improved by treatment with GEM (89.6 ± 21.8 days; $p = 0.0474$) (Fig. 3). The number of PCNA-stained cancer cells in pancreatic cancer tissue was significantly increased compared with normal pancreatic tissue (Fig. 4a, b). After treatment with gemcitabine, the number of PCNA-stained cancer cells was significantly reduced but still higher than that in normal pancreatic tissue (Fig. 4c).

Alpha-SMA-positive cells and extracellular matrix after gemcitabine treatment

Alpha-SMA immunoreactivity was markedly detected in the stroma of pancreatic cancer tissue. The immunohistochemistry showed that α-SMA expression in pancreatic cancer tissue was significantly reduced after treatment with GEM ($p = 0.03$) (Fig. 5). Moreover, Western blot analysis of α-SMA protein in pancreatic cancer tissue was also significantly reduced by the treatment ($p = 0.001$) (Fig. 6). However, there was no significant difference in Picrosirius red expression in pancreatic cancer tissue between control and GEM-treated animals (Fig. 7).

Growth factor expression in pancreatic tumor

Vascular endothelial growth factor (VEGF) and TGF-β were almost undetectable in normal pancreas by Western blot, but they were strongly expressed in pancreatic cancer tissue. However, the expression of VEGF was significantly reduced by GEM treatment ($p = 0.01$), whereas the expression of TGF-β was not inhibited ($p = 0.41$) (Fig. 8).

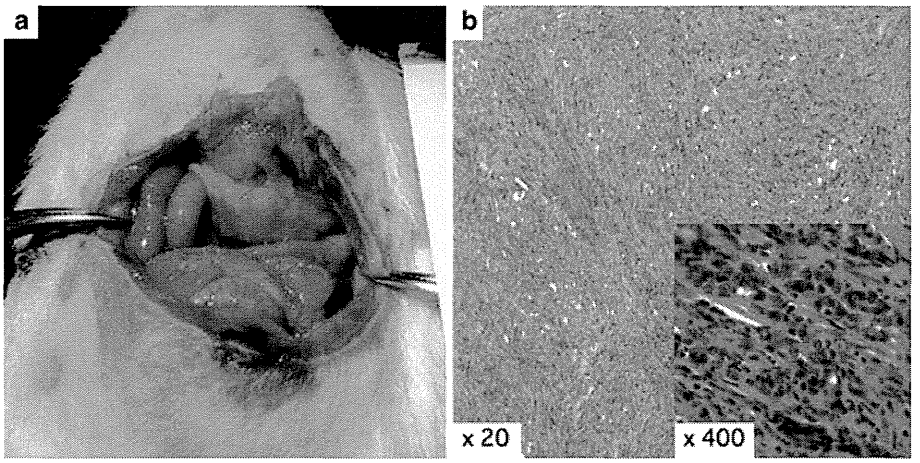

Fig. 2 Gross and microscopic features of orthotopic pancreatic cancer tissue. **a** Gross tumor nodules (4 weeks after implantation). **b** Pancreatic cancer tissue (4 weeks) (×20, ×400, H&E stain)

Discussion

During the last decade, various reports on the interaction between pancreatic cancer cells and PSCs have been published. Growth factors, such as FGF-2, TGF-β1, PDGF, and VEGF, which are secreted by pancreatic cancer cells, activate PSCs. Apte et al. [14] reported that exposure of PSCs to pancreatic cancer cell secretions in vitro resulted in PSC activation, as indicated by significantly increased cell proliferation and α-SMA expression. Furthermore, Bachem et al. [7] reported that pre-incubation of carcinoma cell supernatant with neutralizing antibodies against FGF-2, TGF-β1, and PDGF significantly reduced the PSCs stimulatory effect.

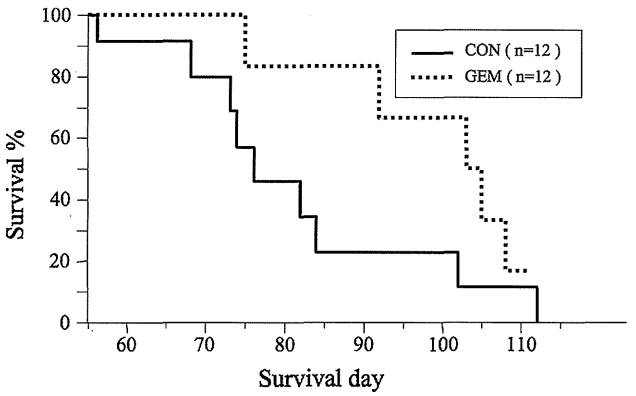

Fig. 3 Overall survival curve for rats with orthotopic pancreatic cancer. The mean animal survival time of the rat pancreatic cancer model (59.6 ± 13.4 days: *black line*) was significantly improved by treatment with GEM (89.6 ± 21.8 days: *dotted line*) ($p = 0.0474$)

Although the above-mentioned studies provided important evidence of stroma–tumor interactions, most of the studies provided the evidence through subcutaneous tumor models or in vitro studies. Several studies using orthotopic pancreatic cancer models have been published in recent years. Most of these models used xenografted, immunoincompetent, or transgenic animals. The rat model that we used in this study was established by Hotz et al. [11], and they reported on a preclinical treatment study using this model [15]. This animal model is immunocompetent and clinically relevant, because syngeneic rat pancreatic cancer cells were orthotopically implanted. Our study showed that the DSL-6A/C1 cells were sensitive to GEM, and that the survival rate of this pancreatic cancer animal model was increased by treatment with GEM.

Interestingly, the expression of α-SMA in the pancreatic cancer tissue was significantly decreased by treatment with GEM. It is considered likely that the activity of α-SMA-positive MCs was inhibited, as demonstrated by the results of immunohistochemistry and Western blot. Because we initially grew the tumor in the subcutis before transplanting it into pancreas parenchyma in this pancreatic cancer model, MCs derived from the subcutis may have been included. However, as the tumor grew, the PSCs are also

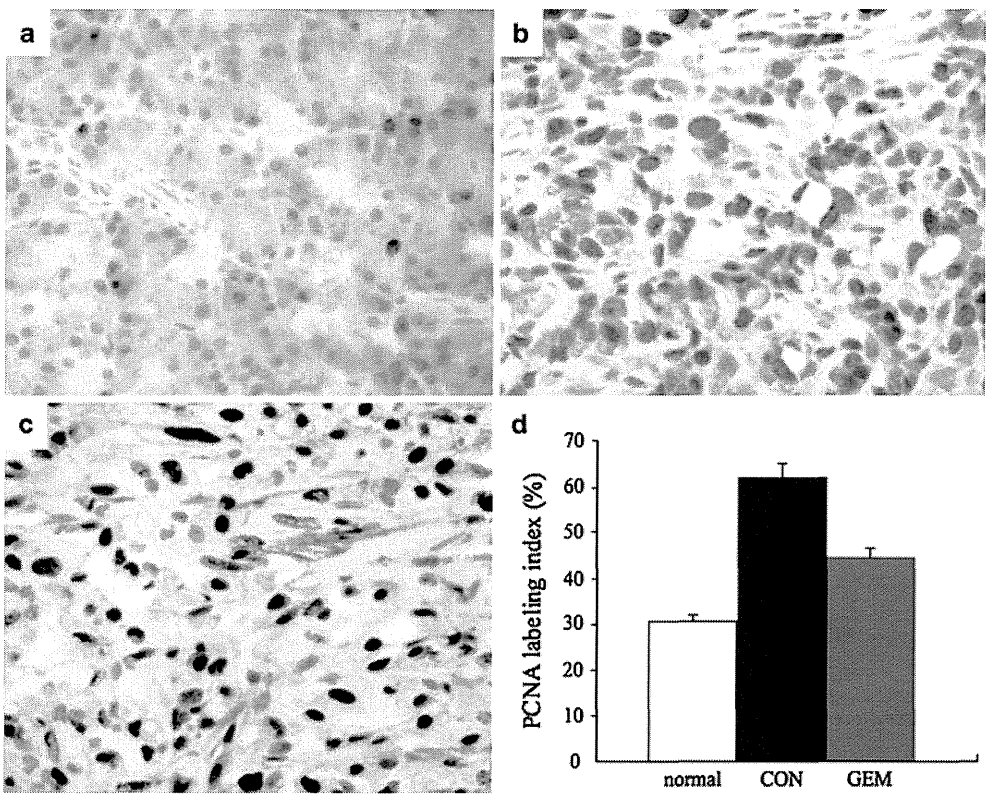

Fig. 4 Immunostaining for PCNA of the pancreatic tissue. PCNA (*brown*) showed the proliferating cells during the late G1 to S phase of the cell cycle. **a** Normal rat pancreatic tissue. **b** No treatment group (control). **c** GEM-treated group (×400). **d** PCNA labeling index shows that the number of PCNA-stained cancer cells after treatment with GEM (*gray bar*) was significantly reduced compared with the control (*black bar*), which still has a higher range than normal pancreatic tissue (*white bar*) (color figure online)

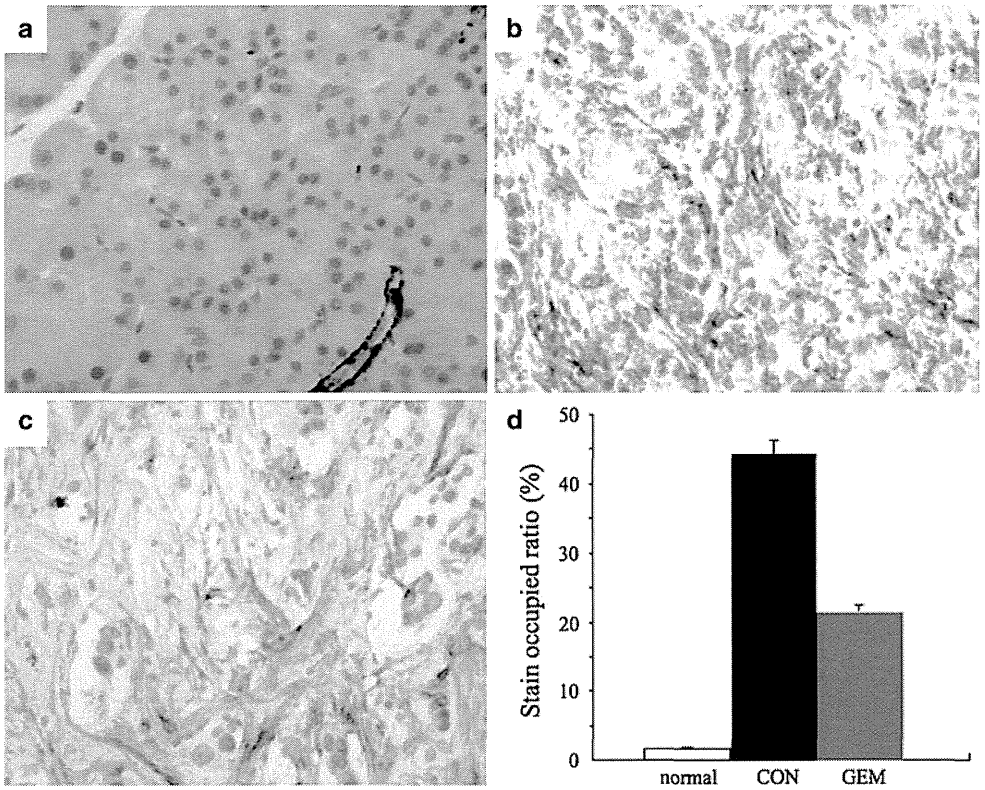

Fig. 5 Immunostaining for α-SMA of the pancreatic tissue. **a** Normal rat pancreatic tissue. **b** No treatment group (control). **c** GEM-treated group (×400). **d** Stain occupied ratio shows that α-SMA expression in pancreatic cancer tissue (*black bar*) was significantly reduced after treatment with GEM (*gray bar*) ($p = 0.03$)

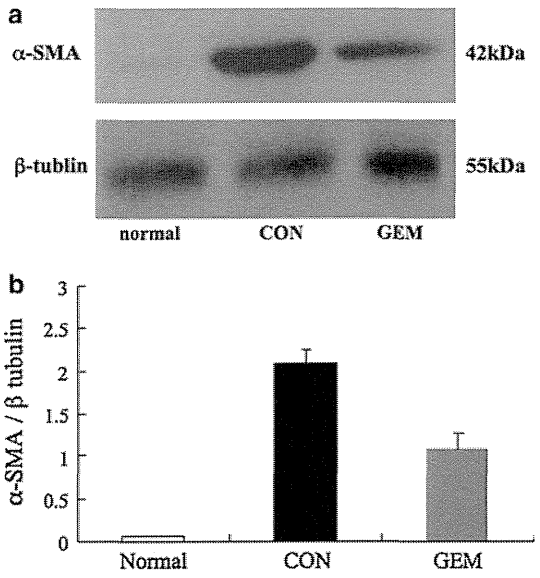

Fig. 6 Western blot analysis of α-SMA protein expression in pancreatic cancer tissue. **a** Western blot analysis of α-SMA protein. *Normal* normal rat pancreatic tissue; *CON* no treatment group (control); *GEM* GEM treated group. **b** Band intensity was quantified and expressed by ratio to β-tubulin ($n = 3$ for each group). Alpha-SMA protein of expression in pancreatic cancer tissue was significantly reduced by treatment with GEM ($p = 0.001$)

thought to migrate into the tumor from pancreatic parenchyma. Erkan et al. [16] have shown that human PSCs are practically resistant to GEM. We have been unable to discover any reports in Medline on direct GEM inhibition of rat PSC activation, but a main reason for this may be that the growth factor secretion by a tumor decreases when the growth of the tumor is being suppressed. We considered that inhibition of activation of α-SMA-positive MCs is not a direct effect of GEM.

Vascular endothelial growth factor plays an important role in tumor angiogenesis. Several reports have demonstrated that patients with pancreatic cancer showing high VEGF expression have significantly shorter survival than patients with lower VEGF expression [17–19]. In this study, we evaluated TGF-β and VEGF, which are well known growth- and PSC-activating factors secreted by pancreatic cancer cells. The expression of TGF-β was not inhibited, but VEGF expression was significantly reduced by GEM treatment. Although pancreatic cancer cells can secrete VEGF, PSCs is one of the principal sources of VEGF in pancreatic cancer tissue [20, 21]. In vitro, hypoxia increased PSC activity and doubled the secretion of periostin, type I collagen, fibronectin, and VEGF [22]. Therefore, we suggest that a decrease of VEGF expression in cancer tissue is caused by an anti-tumor effect of GEM and that inhibition of activation of α-SMA-positive MCs is a secondary effect of tumor cytokines.

Pancreatic cancer is a pathologically unique tumor that is composed of cancer cells and extremely dense desmoplasia containing ECM protein, activated PSCs, and inflammatory cells. Activated PSCs show markedly

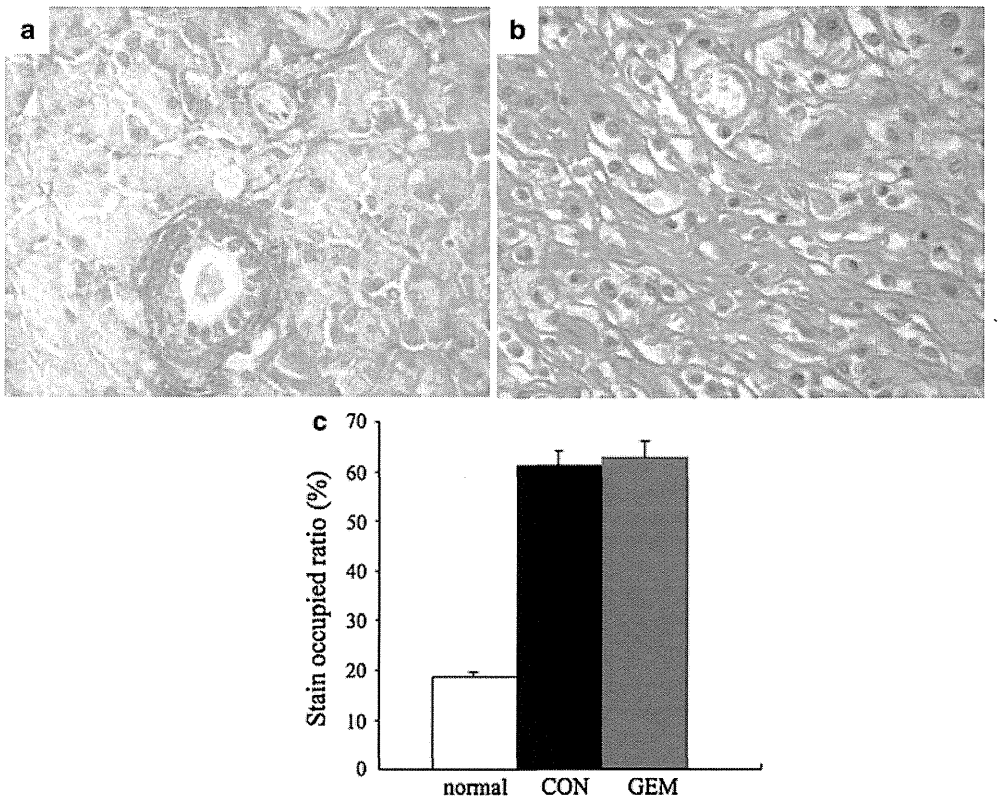

Fig. 7 Picrosirius red staining. **a** Normal pancreatic tissue. **b** Pancreatic cancer tissue (×400). **c** There was no significant difference in Picrosirius red expression in pancreatic cancer tissue between control (*black bar*) and GEM treated animals (*gray bar*)

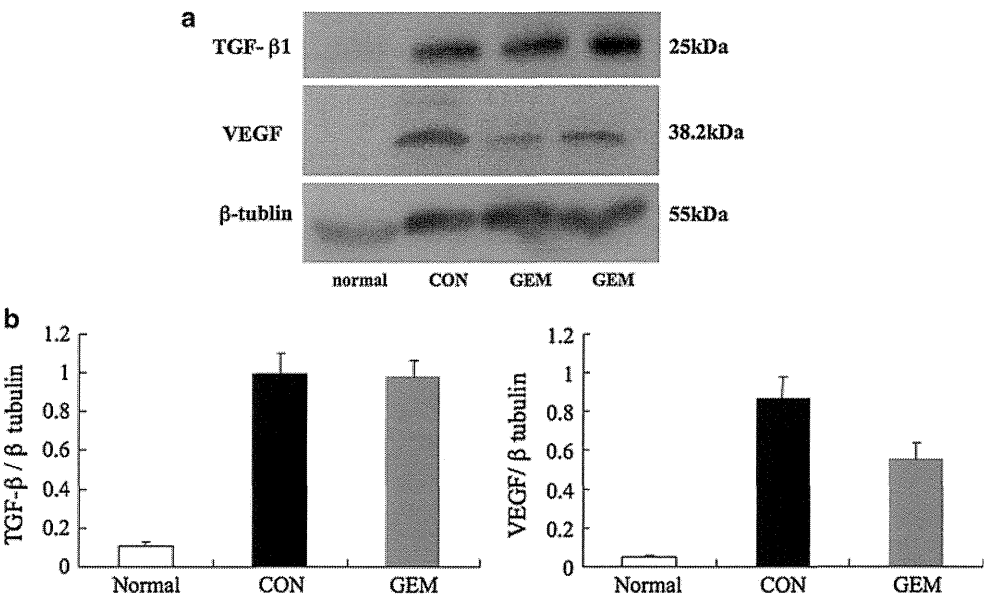

Fig. 8 Western blot analysis of VEGF and TGF-β protein expression in pancreatic cancer tissue. **a** The expression of TGF-β and VEGF in pancreatic cancer tissue. Each lane of GEM represents a different animal. *Normal* normal rat pancreatic tissue; *CON* no treatment group (control); *GEM* GEM treated group. **b** Band intensity was quantified and expressed by ratio to β-tubulin ($n = 3$ for each group). The expression of VEGF was significantly reduced by GEM treatment ($p = 0.01$), but the expression of TGF-β was not inhibited ($p = 0.41$)

increased ECM protein synthesis in response to various stimuli, such as cytokines and growth factors [5, 6], which results in pancreatic fibrosis and a hypoxic microenvironment. Our study showed that the activity of α-SMA-positive MCs in the pancreatic cancer tissue was inhibited by treatment with GEM, but the quantity of ECM did not change. Fibrosis due to chronic pancreatitis was irreversible, as shown in an earlier report [23], and also in our study. There was no change in ECM volume even if the activation of α-SMA-positive MCs, which play a pivotal role in fibrosis in pancreatic cancer tissue, was inhibited.

In summary, when pancreatic cancer growth was suppressed by GEM chemotherapy, activation of α-SMA-positive MCs in the pancreatic cancer tissue was inhibited, and the secretion of VEGF decreased but not secretion of TGF-β1. The decrease of VEGF secretion may be caused

by synergy between the suppression of the cancer cell proliferation and the suppression of activation of α-SMA-positive MCs. Even if the activity of α-SMA-positive MCs decreased, the fibrosis in the pancreatic cancer tissue was irreversible. In conclusion, GEM may not only suppress the tumor cell proliferation, but also favor the suppression of PSCs through VEGF reduction. We suggest that perhaps inhibition therapy of PSC activation in addition to chemotherapy might be a more effective strategy in pancreatic cancer treatment.

Conflict of interest None.

References

1. Apte MV, Haber PS, Applegate TL, Norton ID, McCaoughan GW, Korsten MA, et al. Periacinar stellate shaped cells in rat pancreas: identification, isolation, and culture. Gut. 1998;43:128–33.
2. Apte MV, Haber PS, Darby SJ, Rodgers SC, McCoughan GW, Korsten MA, et al. Pancreatic stellate cells are activated by proinflammatory cytokines: implications for pancreatic fibrogenesis. Gut. 1999;44:534–41.
3. Bachem MG, Schneider E, Gross H, Weidenbach H, Schmid RM, Menke A, et al. Identification, culture, and characterization of pancreatic stellate cells in rats and humans. Gastroenterology. 1998;115:421–32.
4. Haber PS, Keogh GW, Apte MV, Moran CS, Stewaart NL, Crawford DH, et al. Activation of pancreatic stellate cells in human and experimental pancreatic fibrosis. Am J Pathol. 1999;155:1087–95.
5. Jaster R. Molecular regulation of pancreatic stellate cell function. Mol Cancer. 2004;3:26–33.
6. Omary MB, Lugea A, Lowe AW, Pandol SJ. The pancreatic stellate cell: a star on the rise in pancreatic diseases. J Clin Invest. 2007;117:50–9.
7. Bachem MG, Schunemann M, Ramadani M, Siech M, Beger H, Buck A, et al. Pancreatic carcinoma cells induce fibrosis by stimulating proliferation and matrix synthesis of stellate cells. Gastroenterology. 2005;128:907–21.
8. Fujita H, Ohuchida K, Mizumoto K, Egami T, Miyoshi K, Moriyama T, et al. Tumor–stromal interactions with direct cell contacts enhance proliferation of human pancreatic carcinoma cells. Cancer Sci. 2009;100:2309–17.
9. Fujita H, Ohuchida K, Mizumoto K, Nakata K, Yu J, Kayashima T, et al. Alpha-smooth muscle actin expressing stroma promotes an aggressive tumor biology in pancreatic ductal adenocarcinoma. Pancreas. 2010;39:1254–62.
10. Pettengill OS, Faris RA, Bell RHJ, Kuhlmann ET, Longnecker DS. Derivation of duct-like cell lines from a transplantable acinar cell carcinoma of the rat pancreas. Am J Pathol. 1993;143:292–303.
11. Hotz HG, Reber HA, Hotz B, Foitzik T, Buhr HJ, Cortina G, et al. An improved clinical model of orthotopic pancreatic cancer in immunocompetent Lewis rats. Pancreas 2001;22:113–121.
12. Puchtler H, Waldrop FS, Valentine LS. Polarization microscopic studies of connective tissue stained with picro-sirius red FBA. Beitr Path. 1973;150:174–87.
13. Zeng WJ, Liu GY, Xu J, Zhou XD, Zhang YE, Zhang N. Pathological characteristics, PCNA labeling index and DNA index in prognostic evaluation of patients with moderately differentiated hepatocellular carcinoma. World J Gastroenterol. 2002;8:1040–4.
14. Apte MV, Park S, Phillips PA, Santucci N, Goldstein D, Kumar RK, et al. Desmoplastic reaction in pancreatic cancer: role of pancreatic stellate cells. Pancreas. 2004;29:179–87.
15. Hotz B, Buhr HJ, Hotz HG. Intravital microscopic characterization of suramin effects in an orthotopic immunocompetent rat model of pancreatic cancer. J Gastrointest Surg. 2008;12:900–6.
16. Erkan M, Kleeff J, Gorbachevski A, Reiser C, Mitkus T, Esposito I, et al. Periostin creates a tumor-supportive microenvironment in the pancreas by sustaining fibrogenic stellate cell activity. Gastroenterology. 2007;132:1447–64.
17. Seo Y, Baba H, Fukuda T, Takashima M, Sugimachi K. High expression of vascular endothelial growth factor is associated with liver metastasis and a poor prognosis for patients with ductal pancreatic adenocarcinoma. Cancer. 2000;88:2239–45.
18. Ikeda N, Adachi M, Taki T, Huang C, Hashida H, Takabayashi M, et al. Prognostic significance of angiogenesis in human pancreatic cancer. Br J Cancer. 1999;79:1553–63.
19. Knoll MR, Rudnitzki D, Sturm J, Manegold BC, Post S, Jaeger TM. Correlation of postoperative survival and angiogenic growth factors in pancreatic carcinoma. Hepatogastroenterology. 2001;48:1162–5.
20. Masamune A, Kikuta K, Watanabe T, Satoh K, Hirota M, Shimosegawa T. Hypoxia stimulates pancreatic stellate cells to induce fibrosis and angiogenesis in pancreatic cancer. Am J Physiol Gastrointest Liver Physiol. 2008;295:G709–17.
21. Fukumura D, Xavier R, Sugiura T, Chen Y, Park EC, Lu N, et al. Tumor induction of VEGF promoter activity in stromal cells. Cell. 1998;94:715–25.
22. Erkan M, Reiser-Erkan C, Michalski CW, Deucker S, Sauliunatite D, Streit S, et al. Cancer–stellate cell interactions perpetuate the hypoxia-fibrosis cycle in pancreatic ductal adenocarcinoma. Neoplasia. 2009;11:497–508.
23. Raimondi S, Lowenfels AB, Morselli-Labate AM, Maisonneuve P, Pezzilli R. Pancreatic cancer in chronic pancreatitis; aetiology, incidence, and early detection. Best Pract Res Clin Gastroenterol. 2010;24:349–58.

OncoTargets and Therapy

Dovepress
open access to scientific and medical research

Open Access Full Text Article

ORIGINAL RESEARCH

Bevacizumab in the treatment of five patients with breast cancer and brain metastases: Japan Breast Cancer Research Network-07 trial

Daigo Yamamoto[1,3]
Satoru Iwase[2]
Yu Tsubota[1]
Noriko Sueoka[1]
Chizuko Yamamoto[3]
Kaoru Kitamura[4]
Hiroki Odagiri[5]
Yoshinori Nagumo[6]

[1]Department of Surgery, Kansai Medical University, Hirakata, Osaka, [2]Department of Palliative Medicine, University of Tokyo Hospital, Tokyo, [3]Department of Internal Medicine, Seiko Hospital, Neyagawa, Osaka, [4]Breast Unit, Nagumo Clinic, Fukuoka, [5]Department of Surgery, Hirosaki National Hospital, Hirosaki, [6]Breast Unit, Nagumo Clinic, Tokyo, Japan

Background: Brain metastases from breast cancer occur in 20%–40% of patients, and the frequency has increased over time. New radiosensitizers and cytotoxic or cytostatic agents, and innovative techniques of drug delivery are still under investigation.

Methods: Five patients with brain metastases who did not respond to whole-brain radiotherapy and then received bevacizumab combined with paclitaxel were identified using our database of records between 2011 and 2012. The clinicopathological data and outcomes for these patients were then reviewed.

Results: The median time to disease progression was 86 days. Of five patients, two (40%) achieved a partial response, two had stable disease, and one had progressive disease. In addition, one patient with brain metastases had ptosis and diplopia due to metastases of the right extraocular muscles. However, not only the brain metastases, but also the ptosis and diplopia began to disappear after 1 month of treatment. The most common treatment-related adverse events (all grades) were hypertension (60%), neuropathy (40%), and proteinuria (20%). No grade 3 toxicity was seen. No intracranial hemorrhage was observed.

Conclusion: We present five patients with breast cancer and brain metastases, with benefits from systemic chemotherapy when combined with bevacizumab.

Keywords: brain, bevacizumab, metastatic breast cancer

Introduction

Breast carcinoma is the most frequent neoplasia in the US, Europe, and even Japan.[1] Approximately 40%–45% of all patients with breast cancer will develop metastasis, and the mean survival time from the diagnosis of recurrence for these patients is 18–30 months.[2] Therefore, treatment of patients with metastatic breast cancer aims to prolong survival while relieving symptoms and maintaining a good quality of life.[1–4] Brain metastases from breast cancer occur in 20%–40% of patients, and the frequency has increased over time. As a treatment, the combination of surgery and whole-brain radiotherapy is well known and useful, but is still limited. New radiosensitizers and cytotoxic or cytostatic agents and innovative techniques of drug delivery are being investigated.[5]

Bevacizumab has selective activity against the vascular endothelial growth factor (VEGF)-A ligand and has proven to be efficacious when combined with paclitaxel.[6] It has been well documented that tumor blood vessels show increased vascular permeability and interstitial fluid pressure, decreased pericyte coverage, and increased occurrence of tumor hypoxia, further upregulating VEGF production. Therefore, inhibition of

Correspondence: Daigo Yamamoto
Department of Surgery,
Kansai Medical University, Hirakata,
Osaka 570-8507, Japan
Tel +81 72 804 0101
Fax +81 72 804 0170
Email yamamotd@hirakata.ac.jp

VEGF by bevacizumab will not only affect endothelial cells but also the tumor vasculature, suppressing new blood vessel growth and the existing vasculature.

Cautious use of bevacizumab has been recommended in patients at risk of bleeding and uncontrolled hypertension, as well as in patients with a history of arterial thrombotic events. Patients with central nervous system metastases have until recently been routinely excluded from bevacizumab trials, following a single case in 1997 of a 29-year-old patient with hepatocellular carcinoma who experienced a fatal cerebral hemorrhage from a previously undiagnosed brain metastasis in a Phase I study of bevacizumab.[7] However, bevacizumab recently gained accelerated approval from the US Food and Drug Administration for progressive primary brain tumors, with a low rate (approximately 3%) of intratumoral hemorrhage.[8,9] More recent studies showed that bevacizumab is safe in patients with brain metastases.[10–13] We present here the efficacy and side effects of bevacizumab for patients with breast cancer and brain metastases.

Materials and methods

From the Japan Breast Cancer Research Network database, we retrospectively identified five patients treated with bevacizumab-containing chemotherapy regimens for active central nervous system metastases. All patients had recurrent tumors after receiving radiation therapy. All patients received bevacizumab at a dose of 10 mg/kg by intravenous infusion every 2 weeks with concomitant paclitaxel. Paclitaxel 80 mg/m^2 was administered intravenously on days 1, 8, and 15 every 4 weeks. Dose reductions of paclitaxel from 80 to 60 mg/m^2 were performed as described previously.[14] Tumor response was determined by comparing measurements from consecutive magnetic resonance imaging (MRI) scans, as described elsewhere.[8] In brief, progressive disease was deemed to be present if a new lesion had occurred, if the MRI showed a >25% increase in fluid attenuated inversion recovery (FLAIR) or contrast-enhanced volume, or if the MRI scan showed an increase in tumor volume; partial response was defined as a >25% decrease in the enhanced lesion and FLAIR; and a complete response was defined as no detectable contrast enhancement and stable or improved FLAIR signal. Physical examination findings, tumor characteristics, number of treatment cycles, chemotherapy-related toxicities, and symptom severity were recorded every week. Toxicity was graded using the National Cancer Institute Common Terminology Criteria for Adverse Events version 3.0.

Results

Patient characteristics

The characteristics of the study population are presented in Table 1. The median age was 60 (range 39–71) years. Eastern Cooperative Oncology Group performance status was <3. All patients were pretreated with whole-brain radiotherapy. The median number of metastatic sites was three (range 1–5).

Efficacy

The patients were evaluable for response and toxicity. Of the five patients, two (40%) achieved a partial response, two had stable disease, and one had progressive disease. Representative data are shown in Figures 1–4. In addition, one patient with brain metastases had ptosis and diplopia due to metastases of the right extraocular muscles (Figures 4 and 5). However, not only the brain metastases but also the ptosis and diplopia began to disappear after 1 month of treatment (Figure 5). Median time to disease progression was 86 (range 30–135) days. Two patients (40%) were still alive at the last follow-up.

Safety

The most common treatment-related adverse events were grade 1/2 in intensity. Common toxicities were

Table 1 Patient characteristics

Patients (n = 5)	
Age, years, median (range)	60 (39–71)
Performance status	
0	0
1	2
2	2
Hormone status	
+	3
–	2
HER2 status	
+	1
–	4
Menopausal status	
Pre	2
Post	3
Type of prior chemotherapy	
Trastuzumab	1
Taxane	4
Anthracycline/taxane	1
Whole-brain radiotherapy	
+	5
–	0
Median number of brain metastatic sites (range)	3 (1–5)
Metastatic sites involved	
Bone/soft tissue	2
Visceral	2

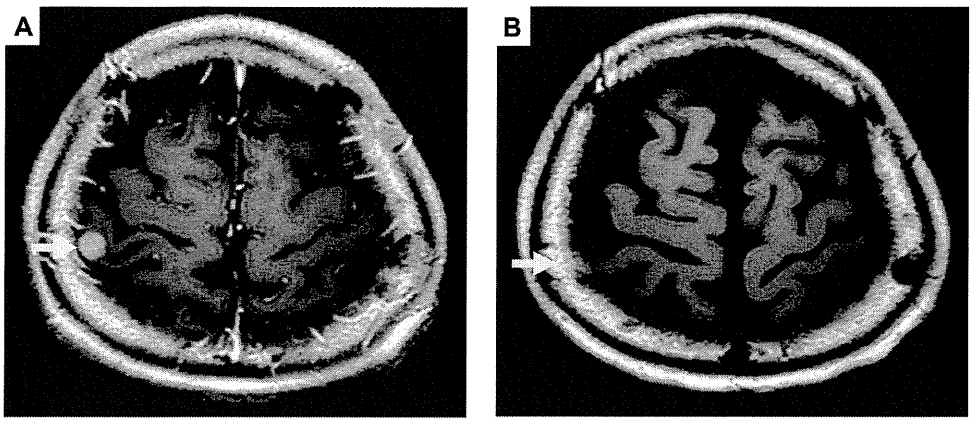

Figure 1 Pre (**A**) and post (**B**) treatment brain magnetic resonance imaging of metastatic tumor showing a partial response (arrows).

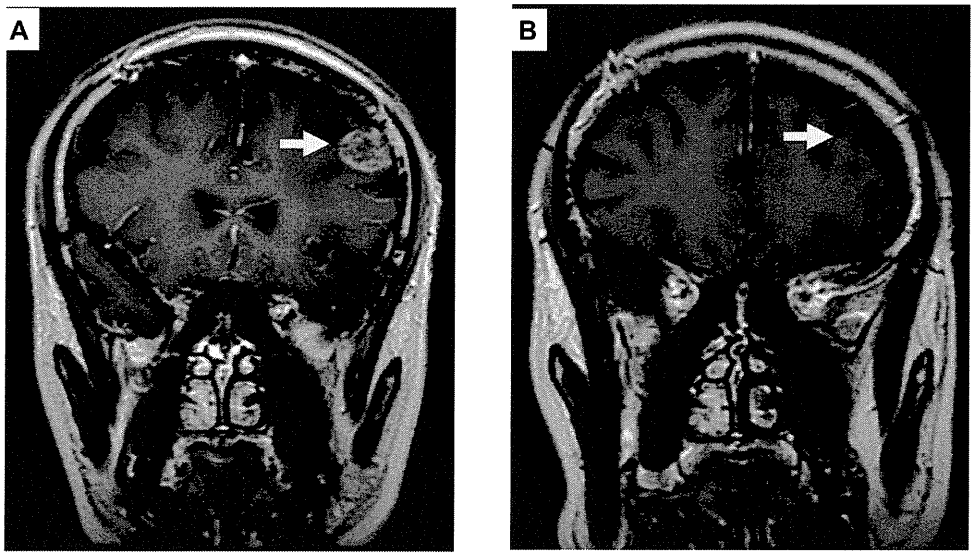

Figure 2 Pre (**A**) and post (**B**) treatment brain magnetic resonance imaging of metastatic tumor showing a complete response (arrows).

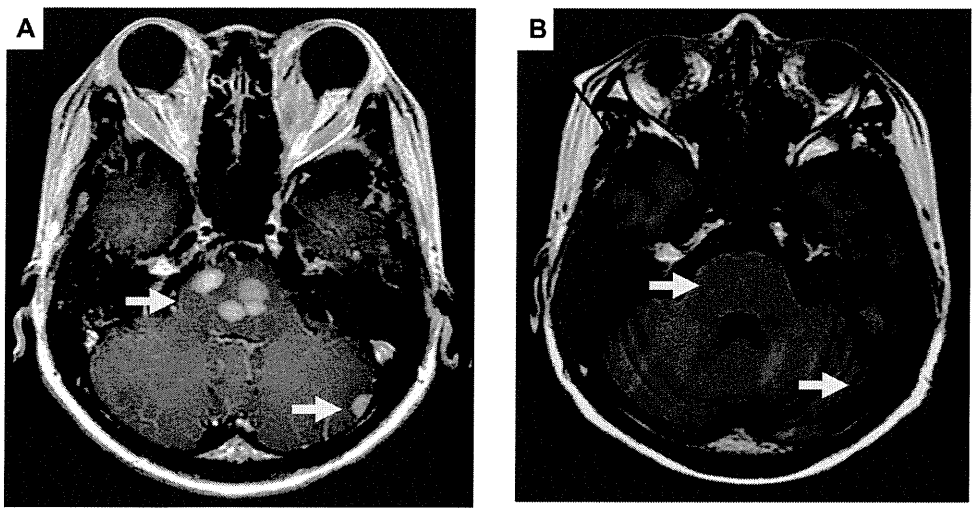

Figure 3 Pre (**A**) and post (**B**) treatment brain magnetic resonance imaging of metastatic tumor showing a partial response (arrows).

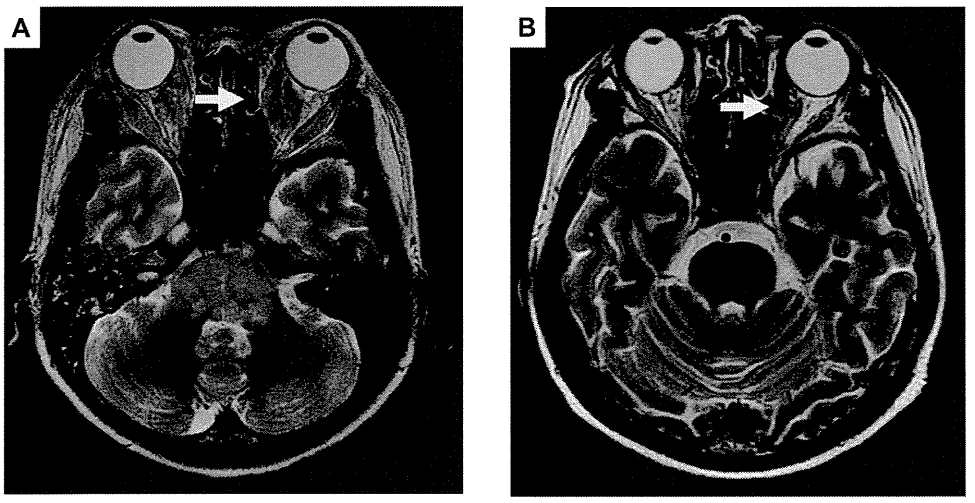

Figure 4 Pre (**A**) and post (**B**) treatment brain magnetic resonance imaging of metastases of right extraocular muscles showing a partial response (arrows).

grade 1 hypertension (60%), grade 1 neuropathy (40%), and proteinuria (20%). No grade 3 toxicity was seen. No intracranial hemorrhage was observed.

Discussion

The results of this multicenter retrospective study suggest that bevacizumab combined with a taxane is highly active and well tolerated by women with breast cancer and brain metastases who have failed whole-brain radiotherapy. Bevacizumab combined with a taxane yielded a 40% response rate. The median time to disease progression was 86 days. The results presented here are similar to those reported elsewhere.[12] The exact mechanism of bevacizumab in brain parenchymal disease is unknown; whether it is a result of direct effects on the tumor vasculature and/or the blood–brain barrier itself is unclear. Most drugs fail to enter the central nervous system because of the blood–brain barrier. This restriction particularly affects drugs that are not substrates for active transport into the central nervous system, hydrophilic molecules larger than 500 Da, and high molecular weight therapeutic modalities, such as monoclonal antibodies, antisense oligonucleotides, viral vectors, stem cells, and nanoparticles.[15] However, some studies have shown that VEGF may provide new opportunities for manipulating the permeability of the blood–brain barrier in vivo.[16,17] Further, previous studies in glioma models have demonstrated a fine balance between VEGF and angiopoietin-2, a proapoptotic factor in angiogenesis.[18] It has been noted that the blood–brain barrier is abnormal with tumors > 0.5 mm, and might affect the integrity of astrocytes and the endothelial cells of the blood–brain barrier.[19] Larger tumors result in an increased risk of ischemia, further disrupting the blood–brain barrier.[20] Additional studies are in progress to evaluate the role of bevacizumab in combination with chemotherapy in previously treated brain metastases originating from non-small-cell lung cancer and also in reducing central nervous system side effects after radiotherapy in patients with primary brain, melanoma, and head and neck cancer.[21,22] In the present study, bevacizumab and paclitaxel suppressed brain metastasis. Therefore, theoretically, there is a possibility that bevacizumab might cross the blood–brain barrier and penetrate brain tumors in sufficient concentrations to synergize with anticancer drugs.

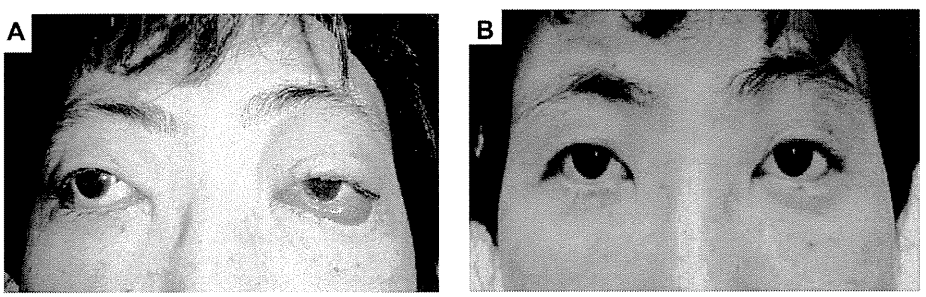

Figure 5 Facial features pre (**A**) and post (**B**) treatment.
Note: Ptosis and diplopia begin to disappear after 1 month of the treatment.

In the current study, the majority of adverse events were mild to moderate in intensity, and confirm the results of previous studies in similar patient populations.[11–13] Acute toxicities were quite mild and manageable. Hypertension and proteinuria were common, and neuropathy was managed with modification of the paclitaxel dose. Further, intracranial hemorrhage was not observed. The limitations of the present study include its retrospective nature and the small number of patients included. Nonetheless, the finding that bevacizumab has significant activity against breast cancer with brain metastasis is important.

Acknowledgment

The authors are indebted to Mr Ito and Mr Yamaga from Chugai Pharmaceutical Co, Ltd.

Disclosure

The authors report no conflicts of interest in this work.

References

1. Shin HR, Boniol M, Joubert C, et al. Secular trends in breast cancer mortality in five East Asian populations: Hong Kong, Japan, Korea, Singapore and Taiwan. *Cancer Sci*. 2010;101:1141–1246.
2. Perez EA. Current management of metastatic breast cancer. *Semin Oncol*. 1999;26:1–10.
3. Kawaguchi T, Iwase S, Takeuchi H, et al. Chemotherapy with low-dose capecitabine as palliative treatment in a patient with metastatic breast cancer: a case report. *Cases J*. 2009;24:9081.
4. Hortobagyi GN. Treatment of breast cancer. *N Engl J Med*. 1998;339:974–984.
5. Tsao MN, Lloyd N, Wong RK, et al. Whole brain radiotherapy for the treatment of newly diagnosed multiple brain metastases. *Cochrane Database Syst Rev*. 2012;4:CD003869.
6. Croom KF, Dhillon S. Bevacizumab: a review of its use in combination with paclitaxel or capecitabine as first-line therapy for HER2-negative metastatic breast cancer. *Drugs*. 2011;71:2213–2229.
7. Gordon MS, Margolin K, Talpaz M. Phase I safety and pharmacokinetic study of recombinant human anti-vascular endothelial growth factor in patients with advanced cancer. *J Clin Oncol*. 2001;19:843–850.
8. Friedman HS, Prados MD, Wen PY, et al. Bevacizumab alone and in combination with irinotecan in recurrent glioblastoma. *J Clin Oncol*. 2009;27:4733–4740.
9. Agha CA, Ibrahim S, Hassan A, Elias DA, Fathallah-Shaykh HM. Bevacizumab is active as a single agent against recurrent malignant gliomas. *Anticancer Res*. 2010;30:609–611.
10. Socinski MA, Langer CJ, Huang JE, et al. Safety of bevacizumab in patients with non-small-cell lung cancer and brain metastases. *J Clin Oncol*. 2009;27:5255–5261.
11. Besse B, Lasserre SF, Compton P, Huang J, Augustus S, Rohr UP. Bevacizumab safety in patients with central nervous system metastases. *Clin Cancer Res*. 2010;16:269–278.
12. Labidi SI, Bachelot T, Ray-Coquard I, et al. Bevacizumab and paclitaxel for breast cancer patients with central nervous system metastases: a case series. *Clin Breast Cancer*. 2009;9:118–121.
13. Bhaskara A, Eng C. Bevacizumab in the treatment of a patient with metastatic colorectal carcinoma with brain metastases. *Clin Colorectal Cancer*. 2008;7:65–68.
14. Yamamoto D, Iwase S, Yoshida H, et al. Efficacy of meloxicam in combination with preoperative chemotherapy for breast cancer – Japan Breast Cancer Research Network (JBCRN) 02-1 Trial. *Anticancer Res*. 2011;31:3567–3572.
15. De Boer AG, Gaillard PJ. Strategies to improve drug delivery across the blood–brain barrier. *Clin Pharmacokinet*. 2007;46:553–576.
16. Ferrara N, Gerber HP, LeCouter J. The biology of VEGF and its receptors. *Nat Med*. 2003;9:669–676.
17. Ay I, Francis JW, Brown RH. VEGF increases blood–brain barrier permeability to Evans blue dye and tetanus toxin fragment C but not adeno-associated virus in ALS mice. *Brain Res*. 2008;1234:198–205.
18. Zadeh G, Guha A. Molecular regulators of angiogenesis in the developing nervous system and adult brain tumors. *Int J Oncol*. 2003;23:557–565.
19. Gerstner ER, Fine RL. Increased permeability of the blood–brain barrier to chemotherapy in metastatic brain tumors: establishing a treatment paradigm. *J Clin Oncol*. 2007;25:2306–2312.
20. Dietrich WD, Busto R, Halley M. The importance of brain temperature in alterations of the blood–brain barrier following cerebral ischemia. *J Neuropathol Exp Neurol*. 1990;49:486–497.
21. ClinicalTrials.gov. Bevacizumab in reducing CNS side effects in patients who have undergone radiation therapy to the brain for primary brain tumor, meningioma, or head and neck cancer. Available at: http://clinicaltrials.gov/ct2/results?term=NCT00492089. Accessed August 27, 2012.
22. ClinicalTrials.gov. A study of bevacizumab in combination with first- or second-line therapy in subjects with brain metastases due to non-squamous NSCLC (PASSPORT). Available at: http://clinicaltrials.gov/ct2/results?term=NCT00312728. Accessed August 27, 2012.

Dig Dis Sci (2012) 57:1404–1412
DOI 10.1007/s10620-012-2029-3

ORIGINAL ARTICLE

A Prospective Randomized Controlled Trial of Preoperative Whole-Liver Chemolipiodolization for Hepatocellular Carcinoma

Masaki Kaibori · Noboru Tanigawa · Shuji Kariya · Hiroki Ikeda · Yoshitsugu Nakahashi · Junko Hirohara · Chizu Koreeda · Toshihito Seki · Satoshi Sawada · Kazuichi Okazaki · A-Hon Kwon

Received: 1 April 2011 / Accepted: 4 January 2012 / Published online: 24 January 2012

Abstract
Background We previously reported that preoperative chemolipiodolization of the whole liver is effective for reducing the incidence of postoperative recurrence and prolonging survival in patients with resectable hepatocellular carcinoma (HCC). The present randomized controlled trial was performed to evaluate the influence of preoperative transcatheter arterial chemoembolization (TACE) on survival after the resection of HCC.
Methods Operative results and long-term outcome were prospectively compared among 42 patients who received only selective TACE targeting the tumor (selective group), 39 patients who received TACE targeting the tumor plus chemolipiodolization of the whole liver (whole-liver group), and 43 patients without preoperative TACE or chemolipiodolization (control group).
Results There were no serious side effects of TACE or chemolipiodolization and the operative outcomes did not differ among the three groups. Even though preoperative TACE induced complete tumor necrosis, there were no significant differences in the pattern of intrahepatic recurrence or the time until recurrence among the three groups. There were also no significant differences in disease-free survival or overall survival among the three groups, even among patients with larger tumor size.
Conclusion These results indicate that preoperative selective TACE and whole-liver chemolipiodolization plus TACE do not reduce the incidence of postoperative recurrence or prolong survival in patients with resectable HCC.

Keywords Hepatocellular carcinoma · Preoperative chemolipiodolization · Whole liver · Hepatectomy · Randomized controlled trial

Introduction

Hepatocellular carcinoma (HCC) is the fifth most common cancer worldwide [1]. Although the majority of patients are still found in Asia and Africa, recent studies have shown that the incidence and mortality rate of HCC are rising in North America and Europe [2, 3]. There has been an increase in reports of non-surgical therapeutic options for small HCC, such as percutaneous ethanol injection therapy [4], microwave coagulation therapy [5], and percutaneous radiofrequency ablation (RFA) [6], but there is ongoing controversy regarding the best method of treating small tumors. In Japan, liver transplantation is not a practical option for most HCC patients, because the national health insurance scheme only covers transplantation for patients with decompensated cirrhosis whose tumors fit the Milan criteria. Resection is, therefore, generally the first-line treatment for patients with small tumors and underlying chronic liver disease, but the long-term survival rate after

M. Kaibori (✉) · A.-H. Kwon
Department of Surgery, Kansai Medical University, 2-3-1 Shinmachi, Hirakata, Osaka 573-1191, Japan
e-mail: kaibori@hirakata.kmu.ac.jp

N. Tanigawa · S. Kariya · S. Sawada
Department of Radiology, Kansai Medical University, Hirakata, Osaka 573-1191, Japan

H. Ikeda · Y. Nakahashi · J. Hirohara · C. Koreeda · T. Seki · K. Okazaki
Department of Gastroenterology and Hepatology, Kansai Medical University, Hirakata, Osaka 573-1191, Japan

potentially curative resection of HCC is still unsatisfactory because of the high rate of recurrence [7]. To improve prognosis, it is important to prevent the recurrence of HCC after its initial resection, but standard therapy for intrahepatic metastasis has not yet been developed.

With various improvements in interventional radiology, transcatheter arterial chemoembolization (TACE) has become an increasingly important palliative treatment for HCC. Initially, TACE was only performed for unresectable HCC, as well as for some early tumors that were extremely difficult to resect. More recently, TACE has been used as preoperative adjuvant therapy in patients who have resectable HCC with the hope that it may improve survival [8–13]. Based on the current evidence, however, preoperative TACE is not routinely recommended for patients undergoing hepatectomy to treat resectable HCC [14–16], and TACE may be contraindicated in patients with cirrhosis because it can lead to the progressive deterioration of liver function [14]. Whether preoperative TACE can improve the long-term survival of HCC patients is still unclear, and there have been only three randomized controlled trials evaluating the influence of preoperative TACE on survival [15, 17, 18]. We previously reported that preoperative chemolipiodolization of the entire liver is effective for reducing the incidence of postoperative recurrence and for prolonging survival in patients with resectable HCC [19]. Accordingly, the present randomized controlled trial was conducted to better assess the influence of preoperative TACE combined with whole-liver chemolipiodolization on survival after the resection of HCC.

Patients and Methods

Patients

Between January 2004 and June 2007, 124 patients with HCC underwent curative hepatic resection at our institution. A curative operation was defined as the resection of all detectable tumors. The eligibility criteria for inclusion in this study were as follows: (1) age 20–80 years; (2) a preoperative diagnosis of HCC with no previous treatment; (3) no other malignancies; (4) Child–Pugh score A or B; (5) leukocyte count $\geq$3,000/mm^3; (6) hemoglobin level $\geq$9.5 g/dl; (7) platelet count $\geq$50,000/mm^3; (8) serum creatinine level <1.2 mg/dl; (9) total bilirubin <2.0 mg/dl; (10) local nodular disease without extrahepatic metastasis; and (11) Eastern Cooperative Oncology Group (ECOG) performance status 0–1 [20]. The etiology of HCC (HCV-related or other [HBV-related or non-B, non-C-related]) and the size of the tumor on imaging were taken into consideration when dividing patients into the three groups. The sample size was estimated based on our previously reported 3-year disease-free survival rates in selective and whole-liver groups, being 25 and 60%, respectively [19]. We needed 37 patients in each group for a type I error rate of 5% and a type II error rate of 20% with a two-tailed test. Among the 124 patients, TACE was performed preoperatively in 81. Patients were randomized to receive chemolipiodolization with gelatin sponge (equal to TACE) targeting the tumor (selective group, $n = 42$), chemolipiodolization with gelatin sponge (equal to TACE) targeting the tumor plus chemolipiodolization without gelatin sponge for the non-cancerous liver (whole-liver group, $n = 39$), or no preoperative TACE (control group, $n = 43$). The study protocol was explained to all patients, and they understood that they would be randomly selected for one of the above three groups. All patients gave written informed consent to participation in the trial. They were randomized by the envelope method and were informed of the result of the randomization before angiography. All operations were performed by the same surgeon, who had experience of over 700 hepatic resections. The protocol for this study was approved by the ethics committee of Kansai Medical University. The primary outcome measures were disease-free survival rate and overall survival rate. Secondary outcome measures included procedure-related complications and hospital mortality (Fig. 1).

Chemolipiodolization

A catheter was selectively inserted into the right or left hepatic artery, a segmental artery, or a subsegmental artery by Seldinger's method. In the selective group, TACE was performed via the right hepatic artery in 16 patients, the left hepatic artery in 10 patients, a segmental artery in 9 patients, and a subsegmental artery in 7 patients. In the whole-liver group, TACE (i.e., chemolipiodolization with gelatin sponge) was performed via the right hepatic artery in 18 patients and the left hepatic artery in 13 patients to target the tumor, while chemolipiodolization alone was performed on the non-cancerous side via the left or right hepatic artery. In a further 8 patients, TACE was performed via a right or left subsegmental artery to target the tumor and chemolipiodolization of the non-cancerous liver was performed via the right and left hepatic arteries as the catheter was withdrawn. The selective group was treated with epirubicin (Farmorubicin) at a mean ($\pm$ standard deviation [SD]) dose of 47.0 $\pm$ 17.8 mg, iodized oil (Lipiodol) at a mean volume of 3.8 $\pm$ 2.1 ml, and gelatin sponge particles. In the whole-liver group, epirubicin (28.1 $\pm$ 5.5 mg), Lipiodol (2.9 $\pm$ 1.4 ml), and gelatin sponge particles were used to treat the tumor, while only epirubicin (22.2 $\pm$ 6.2 mg) and Lipiodol (1.9 $\pm$ 0.8 ml) were infused into the non-cancerous liver. In the control group, only angiography was performed.

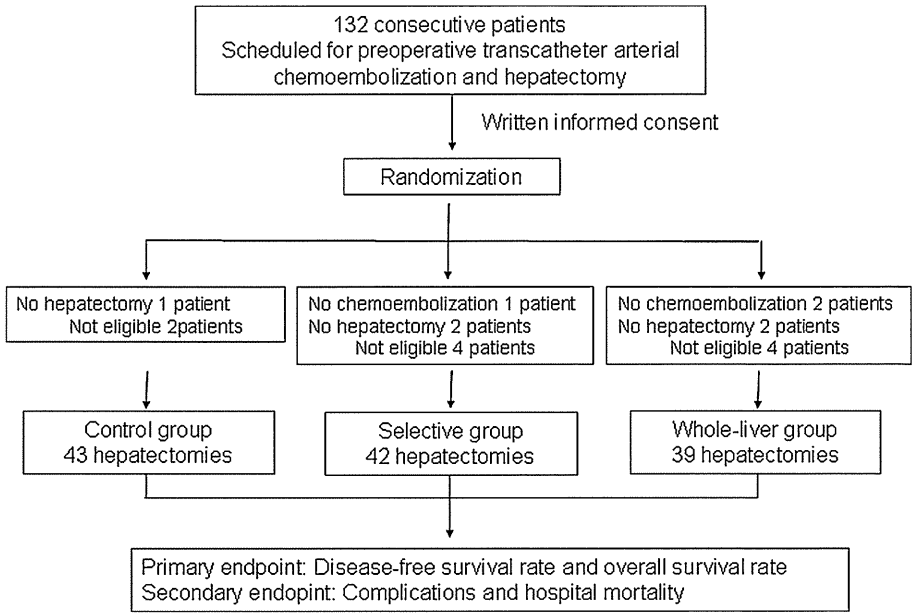

Fig. 1 Study design. We randomly divided patients into three groups: chemolipiodolization with gelatin sponge (equal to transcatheter arterial chemoembolization [TACE]) targeting the tumor (selective group, $n = 42$), chemolipiodolization with gelatin sponge (equal to TACE) targeting the tumor plus chemolipiodolization without gelatin sponge for the non-cancerous liver (whole-liver group, $n = 39$), or no preoperative TACE (control group, $n = 43$)

Clinicopathologic Variables and Surgery

Before randomization, each patient underwent conventional liver function tests, measurement of the indocyanine green retention rate at 15 min (ICGR15), and technetium-99m-diethylenetriamine-pentaacetic acid-galactosyl human serum albumin (^{99m}Tc-GSA) liver scintigraphy [21]. Hepatitis screening was undertaken by testing for hepatitis B surface antigen (HBsAg) and hepatitis C antibody (HCVAb). The levels of α-fetoprotein (AFP) and protein induced by vitamin K absence or antagonist-II (PIVKA-II) were also measured. Surgical procedures were classified according to the Brisbane terminology proposed by Strasberg et al. [22]. In brief, anatomic resection was defined as resection of the tumor together with the related portal vein branches and the corresponding hepatic territory, and was classified as hemihepatectomy (resection of half of the liver), extended hemihepatectomy (hemihepatectomy plus removal of additional contiguous segments), sectionectomy (resection of two Couinaud subsegments [23]), or segmentectomy (resection of one Couinaud subsegment). All of the other procedures were non-anatomic and were classified as limited resection. Peripheral tumors and those with extrahepatic growth were managed by limited resection because this achieved adequate surgical margins. Central tumors located near the hepatic hilum or major vessels were treated by enucleation because it was too difficult or dangerous to remove enough of the liver to obtain an adequate margin. One senior pathologist reviewed all the specimens for histologic confirmation of the diagnosis. The width of the surgical margin was measured from the tumor border to the resection line. We evaluated the extent of necrosis on the largest tumor at its greatest diameter, even in cases with multiple tumors. The tumor stage was defined according to the TNM classification [24].

Follow-Up

Patients who survived were followed up after discharge, with physical examination, liver function tests, and ultrasound, computed tomography (CT), or magnetic resonance imaging being performed at least every 3 months to detect intrahepatic recurrence. Chest radiographs were also obtained to detect pulmonary metastases and chest CT was performed if the plain radiograph showed any abnormalities. Bone metastases were diagnosed by bone scintigraphy.

If the recurrence of HCC was detected by changes in the levels of tumor markers or by imaging, recurrence limited to the remnant liver was treated by TACE, lipiodolization, re-resection, or percutaneous local ablation therapy, such as RFA. If extrahepatic metastases were detected, active treatment was undertaken in patients with good hepatic functional reserve (Child–Pugh class A or B) and good performance status (0 or 1) who had a solitary extrahepatic metastasis and no evidence of intrahepatic recurrence, while other patients were treated only with radiation therapy to control symptoms caused by bone metastases.

Statistical Analysis

The results were expressed as the mean ± SD. Continuous variables were evaluated with the Mann–Whitney *U*-test or the Kruskal–Wallis test, as appropriate. Categorical data were compared with the Chi-square test or Fisher's exact test. The Kaplan–Meier method was used to calculate the

disease-free survival rate and the overall survival rate as of June 2010, and the significance of differences in survival rates was assessed with the generalized log-rank test. In all analyses, $P < 0.05$ was considered to indicate statistical significance.

Results

There were no serious side effects of selective TACE or whole-liver chemolipiodolization. The interval between selective TACE, whole-liver chemolipiodolization, or angiography and hepatic resection was 21.2 ± 10.8, 23.0 ± 13.2, and 20.0 ± 13.2 days, respectively. Table 1 shows the preoperative characteristics of the patients in the three groups. There were no significant differences among the groups with respect to gender, age, Child–Pugh class, etiology of hepatitis or cirrhosis, alcohol abuse, preoperative liver function, or serum AFP and PIVKA-II levels. The operative results and pathologic findings in each group are listed in Table 2. The operating time, blood loss, requirement for transfusion, and operative procedures did not differ significantly among the three groups, nor did the rates of postoperative complications and hospital deaths. There were no significant differences in tumor size or the number of tumors detected on imaging before randomization among the groups. Although the tumor sizes measured in the surgical specimens were smaller in the selective group and the whole-liver group compared with the control group, the differences were not significant. In the selective, whole-liver, and control groups, complete tumor necrosis was confirmed in 9/42 patients (21%), 8/39 patients (21%), and 0/43 patients (0%), respectively. The other pathological characteristics of the tumors were comparable among the three groups.

Recurrence and Survival

The pattern of recurrence and time to recurrence in the three groups are shown in Table 3. A total of 27 patients in the selective group, 28 patients in the whole-liver group, and 26 patients in the control group developed recurrence of HCC. Extrahepatic recurrence was significantly less common in the selective and whole-liver groups compared with the control group. However, the percentage of intrahepatic recurrences due to multinodular/diffuse tumors and the incidence of recurrence within 6 months or 1 year following curative resection were not significantly different among the three groups.

The disease-free survival rates of the entire TACE group (selective and whole-liver groups) and the control group were 65 and 53% at 1 year, and 27 and 32% at 3 years, respectively (Fig. 2a). The overall survival rates of the entire TACE group and the control group were 88 and 83% at 1 year, 75 and 60% at 3 years, and 47 and 56% at 5 years, respectively (Fig. 2b). There were no significant

Table 1 Preoperative clinical characteristics of the three groups

	Control group ($n = 43$)	Selective group ($n = 42$)	Whole-liver group ($n = 39$)	*P*-value
Sex (male/female)	32/11	35/7	30/9	0.5921
Age (years)	66.1 ± 10.6	68.1 ± 5.7	66.8 ± 5.4	0.5122
Child–Pugh class (A/B)	39/4	37/5	34/5	0.8708
Etiology (HBV/HCV/NBC)	11/23/9	4/30/8	6/29/4	0.1663
Alcohol abuse (+/−)	17/26	19/23	19/20	0.6981
Platelet count ($10^4/\mu l$)	18.9 ± 10.6	15.2 ± 7.5	15.1 ± 6.9	0.2448
Total bilirubin (mg/dl)	0.89 ± 0.87	0.86 ± 0.32	0.89 ± 0.41	0.3861
Albumin (g/dl)	3.64 ± 0.57	3.67 ± 0.39	3.50 ± 0.47	0.2804
AST (IU/l)	47 ± 34	46 ± 23	47 ± 21	0.5452
ALT (IU/l)	44 ± 37	40 ± 25	45 ± 23	0.3158
Prothrombin time (%)	89 ± 14	86 ± 13	84 ± 14	0.3568
ALP (U/l)	353 ± 162	346 ± 165	365 ± 144	0.6605
γ-GTP (U/l)	99 ± 69	87 ± 95	101 ± 96	0.1859
ICGR15 (%)	15.5 ± 8.3	19.0 ± 9.5	19.2 ± 9.5	0.1384
GSA Rmax (mg/min)	0.554 ± 0.211	0.505 ± 0.194	0.584 ± 0.277	0.3985
Hyaluronic acid (ng/ml)	175 ± 165	199 ± 226	289 ± 385	0.3140
AFP (ng/ml)	858 ± 5,269	2,432 ± 11,638	1,791 ± 9,898	0.2750
PIVKA-II (mAU/ml)	2,385 ± 9,481	4,845 ± 17,126	1,124 ± 3,970	0.8634

The data represent the mean ± standard deviation (SD) or the number of patients

HBV hepatitis B virus, *HCV* hepatitis C virus, *NBC*, non-hepatitis B or C virus, *AST* aspartate aminotransferase, *ALT* alanine aminotransferase, *ALP* alkaline phosphatase, *γ-GTP* γ-glutamyltransferase, *ICGR15* indocyanine green retention rate at 15 min, *GSA Rmax* maximum removal rate of technetium-99m-diethylenetriamine-pentaacetic acid-galactosyl human serum albumin (^{99m}Tc-GSA), *AFP* α-fetoprotein, *PIVKA-II* protein induced by vitamin K absence or antagonist-II

Table 2 Intraoperative and postoperative characteristics of the three groups

	Control group ($n = 43$)	Selective group ($n = 42$)	Whole-liver group ($n = 39$)	*P*-value
Operating time (min)	321 ± 124	300 ± 100	318 ± 135	0.8368
Operative blood loss (ml)	1,875 ± 1,841	1,418 ± 1,324	1,309 ± 1,218	0.3953
Blood transfusion (+/−)	20/23	15/27	13/26	0.4195
Operative procedure (limited/anatomic resection)	33/10	30/12	29/10	0.8545
No. of patients with complications	8 (19%)	3 (7%)	5 (13%)	0.2888
Hospital death	1 (2%)	1 (2%)	0 (0%)	0.6272
Postoperative hospital stay (days)	20 ± 18	16 ± 5	18 ± 12	0.1685
Tumor size on imaging before TACE (cm)	4.86 ± 4.12	4.30 ± 2.13	4.02 ± 3.88	0.7668
Tumor size in specimen (cm)	4.94 ± 3.52	3.66 ± 1.95	3.45 ± 2.15	0.1610
No. of tumors on imaging before TACE (single/multiple)	34/9	33/9	32/7	0.9156
No. of tumors in specimen (single/multiple)	32/11	32/10	31/8	0.8609
Histology (well/moderately/poorly/complete necrosis)	3/34/6/0	3/30/0/9	1/29/1/8	0.0052
Microscopic capsule (+/−)	38/5	38/4	38/1	0.2940
Microvascular invasion (+/−)	28/15	31/11	24/15	0.4785
Microscopic surgical margin (+/−)	5/38	4/38	2/37	0.5763
Associated liver disease (normal/hepatitis/cirrhosis)	4/28/11	1/27/14	2/24/13	0.6581
Tumor stage (I + II/III + IV)	31/12	31/11	30/9	0.8807

The data represent the mean ± standard deviation (SD) or the number of patients

Table 3 Patterns and timing of recurrence

	Control group ($n = 26$)	Selective group ($n = 27$)	Whole-liver group ($n = 28$)	*P*-value
Extrahepatic recurrence	7/26 (27%)	3/27 (11%)	1/28 (4%)	0.0393
Intrahepatic recurrence				0.8829
Nodular recurrence	6/19 (32%)	6/24 (25%)	8/27 (30%)	
Multinodular/diffuse recurrence	13/19 (68%)	18/24 (75%)	19/27 (70%)	
Timing of recurrence				
≤6 months	7/26 (27%)	6/27 (22%)	4/28 (14%)	0.5128
≤12 months	18/26 (69%)	13/27 (48%)	14/28 (50%)	0.2323

The data represent the number (percentage) of patients

differences in disease-free survival ($P = 0.6603$) or overall survival ($P = 0.4115$) between the two groups. Comparing the three groups, the disease-free survival rates of the selective group, whole-liver group, and control group were 67, 63, and 53% at 1 year, and 29, 27, and 32% at 3 years, respectively (Fig. 3a). The overall survival rates of the selective, whole-liver, and control groups were 91, 84, and 83% at 1 year, and 80, 70, and 60% at 3 years, respectively (Fig. 3b). There were no significant differences in disease-free survival ($P = 0.8303$) or overall survival ($P = 0.7126$) among the three groups.

When only patients with a solitary tumor measuring ≥5 cm in the greatest diameter were analyzed, the disease-free survival rates of the selective, whole-liver, and control groups were 50, 34, and 44% at 1 year, and 10, 11, and 9% at 3 years, respectively ($P = 0.8650$) (Fig. 4a). Among these patients, there were also no differences in the overall survival rate between the selective, whole-liver, and control groups, with survival rates of 82, 79, and 67% at 1 year, and 53, 68, and 47% at 3 years, respectively ($P = 0.7264$) (Fig. 4b).

Discussion

In our previous retrospective study, we found that preoperative chemolipiodolization of the whole liver achieved significant prolongation of both disease-free survival and overall survival for HCC patients [19]. The precise mechanism remains unclear, but some possible explanations are: (1) subclinical micrometastases due to portal vein dissemination or multicentric primary tumors are eliminated by whole-liver therapy and (2) reducing the tumor burden before surgery may lessen the chance of developing resistance to chemotherapy. TACE is a well-recognized treatment for HCC, either as adjuvant therapy or as a

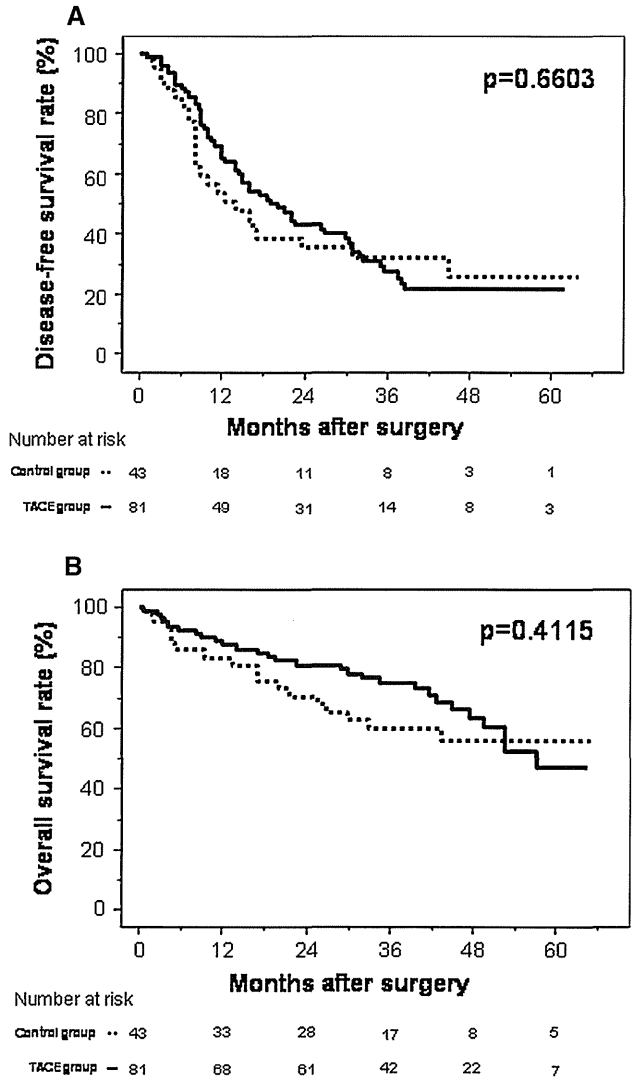

Fig. 2 **a** Comparison of disease-free survival after the resection of hepatocellular carcinoma (HCC) between patients receiving preoperative selective TACE and patients receiving preoperative TACE plus whole-liver chemolipiodolization (entire TACE group, $n = 81$, *solid line*) and patients not receiving preoperative TACE (control group, $n = 43$, *dotted line*). There were no significant differences in disease-free survival between the two groups ($P = 0.6603$). **b** Comparison of overall survival after the resection of HCC between patients receiving preoperative selective TACE and patients receiving preoperative TACE plus whole-liver chemolipiodolization (entire TACE group, $n = 81$, *solid line*) and patients not receiving preoperative TACE (control group, $n = 43$, *dotted line*). There were no significant differences in overall survival between the two groups ($P = 0.4115$)

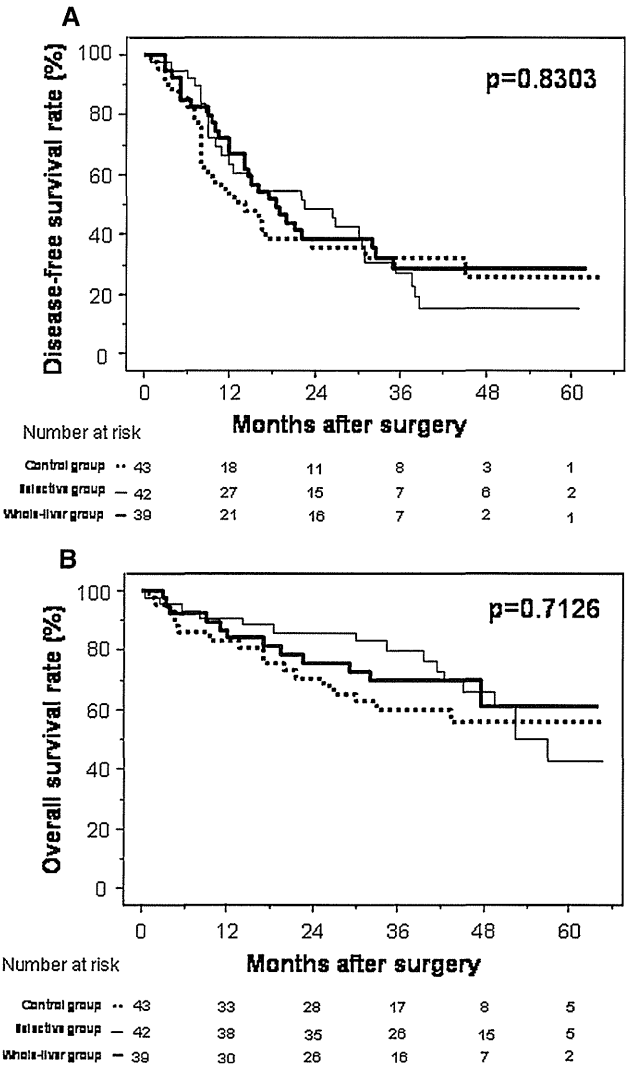

Fig. 3 **a** Comparison of disease-free survival after the resection of HCC among patients receiving preoperative selective TACE (selective group, $n = 42$, *thin solid line*), patients receiving preoperative TACE plus whole-liver chemolipiodolization (whole-liver group, $n = 39$, *thick solid line*), and patients not receiving preoperative TACE (control group, $n = 43$, *dotted line*). There were no significant differences in disease-free survival among the three groups ($P = 0.8303$). **b** Comparison of overall survival after the resection of HCC among the selective group ($n = 42$, *thin solid line*), the whole-liver group ($n = 39$, *thick solid line*), and the control group ($n = 43$, *dotted line*). There were no significant differences in overall survival among the three groups ($P = 0.7126$)

definitive procedure in patients whose tumors are considered to be unresectable [25, 26]. Preoperative TACE is not only intended to prevent recurrence by controlling intrahepatic spread via the portal system, but also to facilitate surgery by reducing tumor bulk. In particular, minimizing resection of the non-tumorous liver is vital in patients with cirrhosis to avoid postoperative hepatic failure. Uchida et al. [14] reported a lower survival rate among cirrhosis patients who underwent TACE prior to the resection of HCC compared with patients who did not undergo TACE, and they recommended against preoperative TACE for patients with cirrhosis because the procedure could accelerate the deterioration of liver function. Lu et al. [11] performed a retrospective analysis of 120 HCC patients and concluded that preoperative TACE might benefit those with tumors >8 cm in diameter, but not those with tumors

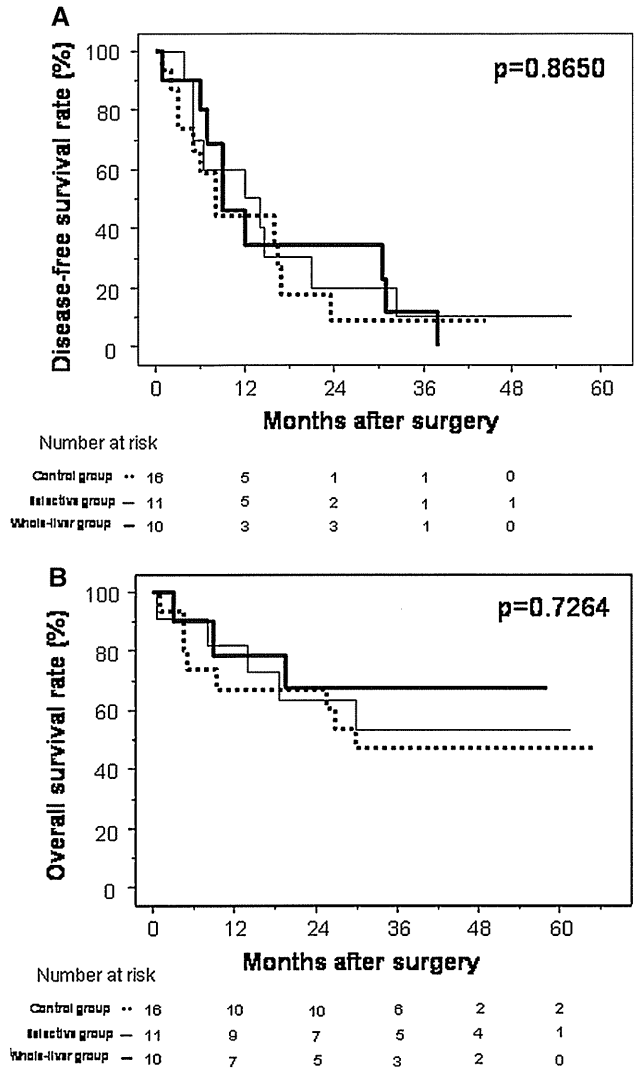

Fig. 4 **a** Comparison of disease-free survival after resection of a solitary HCC ≥5 cm in the greatest diameter among patients receiving preoperative selective TACE (selective group, $n = 11$, *thin solid line*), patients receiving preoperative TACE plus whole-liver chemolipiodolization (whole-liver group, $n = 10$, *thick solid line*), and patients without preoperative TACE (control group, $n = 16$, *dotted line*). There were no significant differences in disease-free survival among the three groups ($P = 0.8650$). **b** Comparison of overall survival after resection of a solitary HCC ≥5 cm in the greatest diameter among the selective group ($n = 11$, *thin solid line*), the whole-liver group ($n = 10$, *thick solid line*), and the control group ($n = 16$, *dotted line*). There were no significant differences in overall survival among the three groups ($P = 0.7264$)

2–8 cm in diameter. In contrast, it was reported that downstaging or total necrosis of the tumor was achieved by preoperative TACE in 62% of 103 HCC patients with cirrhosis, leading to an improvement of disease-free survival after liver resection and liver transplantation [13]. Thus, the value of preoperative TACE is still controversial.

A meta-analysis including seven randomized clinical trials was undertaken in the late 1990s to investigate the usefulness of TACE for treating unresectable HCC, which demonstrated an improvement in 2-year survival (odds ratio 0.53, $P = 0.017$) compared with control patients who were treated conservatively or received suboptimal management [27]. This established the role of TACE as the standard care for unresectable HCC, whether as palliative therapy or to improve resectability [27]. Subsequent investigations were directed towards the preoperative use of TACE as neoadjuvant therapy to prevent recurrence. To assess the clinical efficacy of preoperative TACE for resectable HCC, two randomized trials were conducted in 1995 and 1996 [15, 17] (Table 4). Both of these trials found no improvement in disease-free survival following neoadjuvant TACE, and Wu et al. [17] reported worse overall survival in the TACE group. In 2009, a randomized trial of neoadjuvant TACE for large resectable HCC was reported [18]. The results were similar, with no difference in disease-free survival or overall survival between the groups with or without TACE (Table 4). The present study is the fourth randomized trial to compare the long-term prognosis after the resection of HCC in patients with or without preoperative TACE. However, it is difficult to simply compare these trials. Zhou et al. [18] and Wu et al. [17] enrolled patients with large HCCs, whereas Yamasaki et al. [15] and the current trial enrolled patients with smaller HCCs. In the trial reported by Wu et al. [17], patients who received TACE underwent surgery a mean of 17.9 weeks after the detection of HCC, which was significantly longer than those not receiving TACE, who underwent resection 2.3 weeks after the detection of HCC ($P = 0.009$). In this study, patients in all groups underwent surgery in 20–23 days. Differences in the conclusions of the different trials could be attributed to the differences in the study designs or background characteristics.

We found no significant differences in disease-free survival or overall survival between the entire TACE group (selective and whole-liver groups) and the control group, or among the whole-liver, selective, and control groups, even among patients with tumor size >5 cm (Figs. 2, 3, and 4). The extrahepatic recurrence rate was significantly lower in the selective and whole-liver groups compared with the control group. However, even though preoperative TACE induced complete tumor necrosis, there were no significant differences in the pattern of intrahepatic recurrence or the time until recurrence among the three groups.

In conclusion, preoperative selective TACE or TACE plus whole-liver chemolipiodolization neither reduced the incidence of postoperative recurrence nor prolonged survival in patients with resectable HCC. Thus, despite its safety and feasibility, we cannot recommend preoperative TACE as a routine procedure before hepatectomy in patients with resectable HCC.